Biochemical and Biophysical Research Communications **272,** 586–590 (2000)
doi:10.1006/bbrc.2000.2819, available online at http://www.idealibrary.com on IDEAL®

Direct Observation of Processive Movement by Individual Myosin V Molecules

Takeshi Sakamoto,* Ichiro Amitani,* Etsuo Yokota,† and Toshio Ando*,[1]

**Department of Physics, Faculty of Science, Kanazawa University, Kakuma-machi, Kanazawa, Ishikawa-ken 920-1192, Japan; and †Department of Life Science, Faculty of Science, Himeji Institute of Technology, Himeji 678-1297, Japan*

Received May 1, 2000

Myosin V is an unconventional myosin thought to move processively along actin filaments. To have hard evidence for the high processivity, we sought to observe directly the movement by individual native chick brain myosin V (BMV) molecules with fluorescent calmodulin. Single BMV molecules did exhibit highly processive movement along actin filaments fixed to a coverslip. BMV continued to move up to the barbed end of its actin track, and did not readily detach from action. The barbed end, therefore, got brighter with time, because of a constant stream of BMV traffic. The maximum speed of the processive movement was 1 μm/s, and the maximum actin-activated ATPase rate was 2.4 s^{-1}. These values apparently imply that BMV travels a great distance, 400 nm, per an ATPase cycle.

Key Words: **motor protein; sliding movement; processivity; ATPase; actin; myosin.**

The transport of vesicles and organelles to specific locations is a fundamental process in cells. This process is performed mainly by actin-based and microtubule-based protein motors. Of the unconventional myosin families the class V myosins have been shown to transport synaptic and endoplasmic reticulum vesicles in neurons (1–3), pigment granules in melanocytes (4, 5), and the vacuole in yeast (6, 7). Myosin V consists of two N-terminal heads containing the actin-binding and ATP hydrolysis sites, two extended neck domains each of which contains six IQ motifs, and a tail domain consisting of a coiled-coil region attached to a C-terminal globular region (8–10). The IQ motifs form binding sites for calmodulin (CaM) and related light chains (9–11). Unlike myosin II, the tail does not self-associate, and therefore myosin V does not form filaments (10, 12). The C-terminal globular region is believed to associate with cargo to be carried by myosin V. The cycling rate of the actin-activated ATPase is limited by the ADP-release step, which allows myosin V to spend a large part of the cycle time strongly bound to actin (13, 14). This kinetic nature has not been found yet in the other myosin families.

Based on the cellular functions and the ATPase kinetics, myosin V has been inferred to be a processive motor like the microtubule-based motors, kinesin (15, 16) and dynein (17), that is, a single myosin V molecule may be able to travel long distances along its actin track, repeating its ATPase cycles. The processivity is more directly suggested by a recent observation that actin filaments moved continuously over surfaces coated with BMV (myosin V purified from chick brain) at low densities, and swiveled about a single contact point as they moved (12). Moreover, it was shown in an optical trapping assay that a single molecule of BMV pulled an actin filament successively for three-to-five, not many, steps before being stalled by the optical trapping force (12). In the present study we directly observed movement by individual BMV molecules on fixed actin tracks, and found that BMV travels over a distance of several micrometers without detaching from actin, that is, BMV makes many steps in succession.

MATERIALS AND METHODS

Proteins. BMV was prepared as described (18), stored at 0°C, and used within a week. Actin was prepared from rabbit skeletal muscle, and purified as described (19). Bovine brain CaM and bovine serum albumin (BSA; fraction V) was obtained from Sigma (USA). Streptavidine was obtained from Life Technologies (USA).

Cy3-labeling of calmodulin. After dialyzing against Buffer A (0.3 M KCl, 50 mM boric acid (pH 8.5), 0.1 mM $CaCl_2$), bovine brain CaM (15 μM) was mixed with 30 μM Cy3-Osu (Amersham Pharmacia Biotech, UK) and incubated for 1 h at 25°C. After adding 5 mM dithiothreithol (DTT) to stop the reaction, it was exhaustively dialyzed against Buffer B (25 mM KCl, 20 mM imidazole (pH 7.6), 2 mM $MgCl_2$, 1 mM EGTA) plus 2 mM β-mercaptoethanol (β-ME). The concentration of Cy3 in the Cy3-CaM was estimated by the absorbance at 550 nm and the molar extinction coefficient, 1.5×10^5 $M^{-1}cm^{-1}$.

[1] To whom correspondence should be addressed. Fax: +81 76-264-5739. E-mail: tando@kenroku.kanazawa-u.ac.jp.

0006-291X/00 $35.00

Preparation of Cy3-BMV. BMV (150 nM) was mixed with Cy3-CaM (1.5 μM) in Buffer B plus 5 mM DTT, and incubated for 2 min at 25°C. After adding $CaCl_2$ (final 1.01 mM), the mixture was incubated for 5 min at 25°C, followed by the addition of EGTA (final 4 mM). To remove free Cy3-CaM, the sample was mixed with F-actin (final 1 μM), and centrifuged (148,000*g*, 1 h). The pellet was dissolved in Buffer C (250 mM KCl, 2 mM $MgCl_2$, 1 mM EGTA, 20 mM imidazole (pH 7.6), 5 mM DTT, 2 mM ATP). The acto-Cy3-BMV was applied to a Q-Sepharose (Amersham Pharmacia Biotech, Sweden) column (volume, 400 μl). F-actin was removed from the sample by washing the column with 20 ml of Buffer C. After washing the column with 20 ml of Buffer C without ATP, Cy3-BMV was eluted out with a linear gradient 0.25-1 M KCl with 20 mM imidazole (pH 7.6), 2 mM $MgCl_2$, 1 mM EGTA and 5 mM DTT (total 30 ml), and dialyzed against Buffer B plus 2 mM β-ME.

In vitro actin-filament sliding assay. The assay was according to Toyoshima *et al.* (20), with a slight modification (cover slips for flow cells were treated with 0.2%, instead of 0.1%, nitrocellulose isopentyl acetate solution for 1 min). F-actin was labeled with rhodamine-green phalloidine (RGP). BMV or Cy3-BMV (100 nM, 20 μl) was applied to the flow cell (volume 10–20 μl), and incubated for 2 min. The cell was washed with 200 μl of Buffer B. Then, 50 μl of BSA (1 mg/ml in Buffer B) was put into the cell, which was incubated for 2 min and was washed with Buffer B. RGP-labeled F-actin (8 nM, 100 μl) was applied to the cell and incubated for 2 min. Finally, the buffer solution was replaced with motility buffer containing 20 mM imidazole (pH 7.6), 2 mM $MgCl_2$, 1 mM EGTA, 2 mM β-ME, 2 mM ATP, various concentrations of KCl, and an oxygen-scavenging system (0.2 mg/ml glucose oxidase, 0.36 mg/ml catalase and 4.5 mg/ml glucose). Sliding movement of actin filaments was observed at 25°C using an SIT video camera (C2741-08, Hamamatsu Photonics) connected to an unmodified microscope (Olympus IX70; equipped with an oil-immersion objective, 100s, NA 1.35) with epifluorescence excitation with a high-pressure mercury lamp and a filter set (U-MNIBA; Olympus, Japan). The images were recorded with a Hi8 video cassette recorder (EVO-9659, Sony, Japan). The recorded images were digitized with an image processor (Excel, Nippon Avionics, Japan) and the two-dimensional coordinates of the rear end of each actin filament were chased frame by frame. Length of a track connecting these coordinates during a given period of time was calculated and averaged over more than fifty actin filaments. The sliding velocity was obtained by dividing the average value of the lengths of tracks by the given period of time.

In vitro BMV movement assay. G-actin (10 μM) was mixed with 50 μM biotin-maleimide (Dojindo Laboratories, Japan) in a solution containing 20 mM TES-HCl (pH 7.0), 0.2 mM $CaCl_2$, 0.1 mM NaN_3, 0.2 mM ATP, and incubated for 1 h at 25°C. After adding 5 mM DTT to stop the reaction, the biotinylated G-actin was dialyzed against the same buffer solution. The concentration of biotin incorporated into G-actin was measured as described (19). One-to-one stoichiometric incorporation was achieved. The biotinylated G-actin was copolymerized with nonlabeled G-actin (the molar ratio, 1:200) in Buffer B. This ratio seemed important for observing processive movement by Cy3-BMV. The resulting F-actin was labeled with RGP or phalloidine, and then fixed onto a coverslip as follows. First, BSA was biotinylated with biotin-$(AC_5)_2$-Osu (Dojindo Laboratories, Japan) in a BSA/biotin molar ratio of 1:20 in 0.1 M boric acid, pH 8.8 for 90 min at 25°C, and dialyzed against Buffer B. The sample contained 2 biotins per BSA. The biotin-BSA (10 μM, 20 μl) was applied to a flow cell (volume 10 μl) made of two nitrocellulose-coated coverslips. The cell was incubated for 2 min, and washed with 300 μl of Buffer B. Streptavidin (0.5 mg/ml, 10 μl) dissolved in Buffer B was applied to the cell, and incubated for 3 min. Unattached Streptavidin was washed out with 600 μl of Buffer B. The partially biotinylated F-actin (1 μM, 20 μl) was applied to the cell, and incubated for 2 min. Unattached F-actin was washed out with 200 μl of Buffer B. Finally, Cy3-BMV (1 nM) in 100 μl of motility buffers was applied to the cell. Motility buffers are the same as those used for the actin-filament sliding assay. Fluorescence image of Cy3-BMV was observed using an objective-type total internal reflection fluorescence (OTIRF) video microscope, and recorded with a digital video cassette recorder (DSR-20, Sony, Japan). The two-dimensional coordinates of each Cy3-BMV were chased frame by frame. Length of a track connecting these coordinates during a given period of time was calculated and averaged over more than 100 Cy3-BMV molecules. The sliding velocity was obtained by dividing the average value of the lengths of tracks by the given period of time.

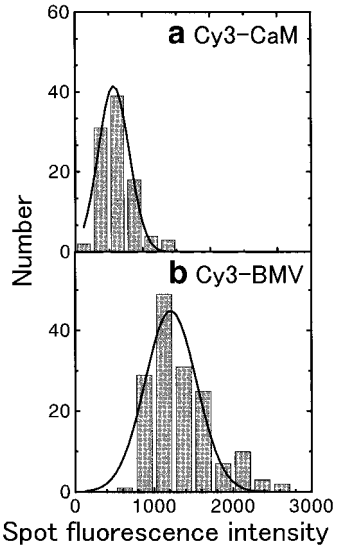

FIG. 1. Distributions of spot intensities (arbitrary units) for (a) Cy3-CaM and (b) Cy3-BMV. The spot intensities were obtained by integrating the intensity over a square (13 × 13 pixels) enclosing the spot and subtracting a background integrated over the same square after complete photobleaching of Cy3.

Microscopy. The OTIRF microscope was constructed as described (21), using an epifluorescence microscope (IX50; Olympus) equipped with an oil-immersion objective lens (PlanApo 100×, NA 1.4) and a relay lens (PE5, 5×; Olympus) connected to an SIT video camera (C2400-08S; Hamamatsu Photonics). The excitation light source is a diode green laser (model 4601-050, 532 nm, 50 mW; Uniphase) attenuated by two 20% neutral density filters.

ATPase assay. Actin-activated BMV and Cy3-BMV ATPase activities were measured at three different [KCl] with nine different actin concentrations. The buffer solution contained 2 mM ATP, 20 mM imidazole (pH 7.6), 2 mM $MgCl_2$, 1 mM EGTA, and KCl (25, 100, or 200 mM). The concentration of BMV or Cy3-BMV was 30–60 nM. Amounts of phosphate liberated at 25°C were quantified by the method of Fiske and Subbarow (22). The ATPase activities were determined by analyzing the amounts of phosphate liberated at seven time points by the least-squares criterion.

F-actin cosedimentation assays. BMV (150 nM) or Cy3-BMV (150 nM) was mixed with 40 μM F-actin at 25°C in 2 mM ATP, 20 mM imidazole (pH 7.6), 2 mM $MgCl_2$, 1 mM EGTA, 2 mM β-ME and three different [KCl] (25 mM, 80 mM, or 150 mM). The samples (200 μl) were then immediately centrifuged (148,000*g*, 45 min, 25°C). The supernatants were carefully aspirated and mixed with 50 μl SDS sample buffer. The pellets were resuspended in the buffer solution (200 μl) plus 50 μl SDS sample buffer. Pellet and supernatant were run on SDS polyacrylamide gels and silver-stained. As a control, it was confirmed that BMV or Cy3-BMV alone was not sedimented, irrespective of the presence of ATP.

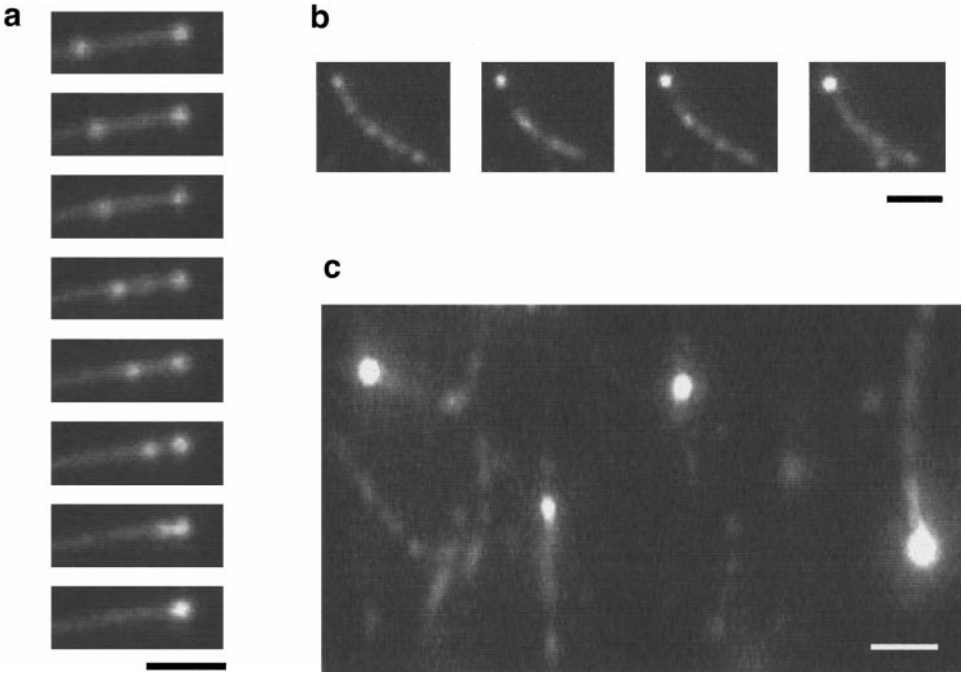

FIG. 2. Processive movement by individual BMV molecules along actin filaments. (a) Successive video images at 0.5-s intervals showing processive movement by a single molecule of BMV along a fluorescent actin filament. The actin filament is labeled with RGP. A light spot in the left-hand side is moving toward the stationary light spot at the actin-filament end. KCl: 75 mM. Scale: 2 μm. (b) Successive video images at 2-s intervals. The barbed end of the actin filament is getting brighter with time because of a constant stream of BMV traffic. A chain of light spots are visible on the actin filament labeled with nonfluorescent phalloidine. KCl: 25 mM. Scale: 2 μm. (c) A video image showing bright spots formed 1 min after incubating BMV in the motility-assay cell. The actin filaments are labeled with nonfluorescent phalloidine. KCl: 25 mM. Scale: 2 μm. The camera gain and the offset levels are different between (a), (b) and (c). In (b) and (c), these parameters for imaging are lower than those in (a). Therefore, we cannot compare the spot intensities in the three cases.

RESULTS AND DISCUSSION

To visualize BMV under the OTIRF microscope we first attempted to label BMV directly with amino-reactive or SH-reactive fluorophores. The labeled BMV, however, did not support *in vitro* actin-filament sliding. So, next, we exploited the property of BMV that calmodulin (CaM) attached to the neck region can dissociate partially in the presence of a micromolar order of Ca^{2+}, and the resulting vacant CaM-binding sites can be refilled when $[Ca^{2+}]$ is returned to a much lower level in the presence of excess amounts of free CaM (10, 11). As the exogenous CaM, we used bovine CaM labeled with a fluorophore, Cy3 (Cy3/CaM = 1.85). In this way a part of the endogenous CaM was successfully replaced with the fluorescent CaM. This sample of BMV contained 4.2 Cy3/BMV, indicating that 2.2 CaMs were replaced on the average. This Cy3-BMV supported *in vitro* motility of actin filaments indistinguishably from that produced by non-labeled BMV (the maximum velocity is 0.55 μm/s). OTIRF video microscopy was employed to observe Cy3-BMV molecules attached to a coverslip. We saw light spots on the monitor. To examine whether these spots represent individual Cy3-BMV molecules, distribution of spot intensities of the Cy3-BMV sample (I_M) was compared with that of Cy3-CaM (I_C) (Fig. 1). The ratio of the mean values, i.e., $\langle I_M \rangle / \langle I_C \rangle$, was 2.1. This value was quite similar to the average number of substituted CaM measured in solution, indicating that Cy3-BMV is not oligomerized. Electron microscopic observation of Cy3-BMV also supported this conclusion (data not shown).

We constructed an *in vitro* BMV motility assay system by attaching partly (0.5%) biotinylated actin filaments onto a streptavidine-coated coverslip. After attaching to an actin filament, Cy3-BMV moved continuously and smoothly on its actin track (Fig. 2a). At [KCl] lower than 100 mM, Cy3-BMV molecules often traveled up to the barbed ends of actin filaments. After reaching the barbed ends, Cy3-BMV did not readily detach from actin. The barbed ends were, therefore, getting brighter with time because of a constant stream of Cy3-BMV traffic (Fig. 2b and 2c). At [KCl] higher than about 150 mM, Cy3-BMV often detached from actin before reaching the barbed end of its actin track. The distance that Cy3-BMV traveled seemed to fit single exponential statistics (Fig. 3a–3d), and decreased with increasing [KCl] (Fig. 3e). The processive movement was still visible even at 400 mM KCl, although the mean travel distance was small (about 660 nm). The rate of movement was 0.54 μm/s at 25 mM KCl, increased moderately with increasing

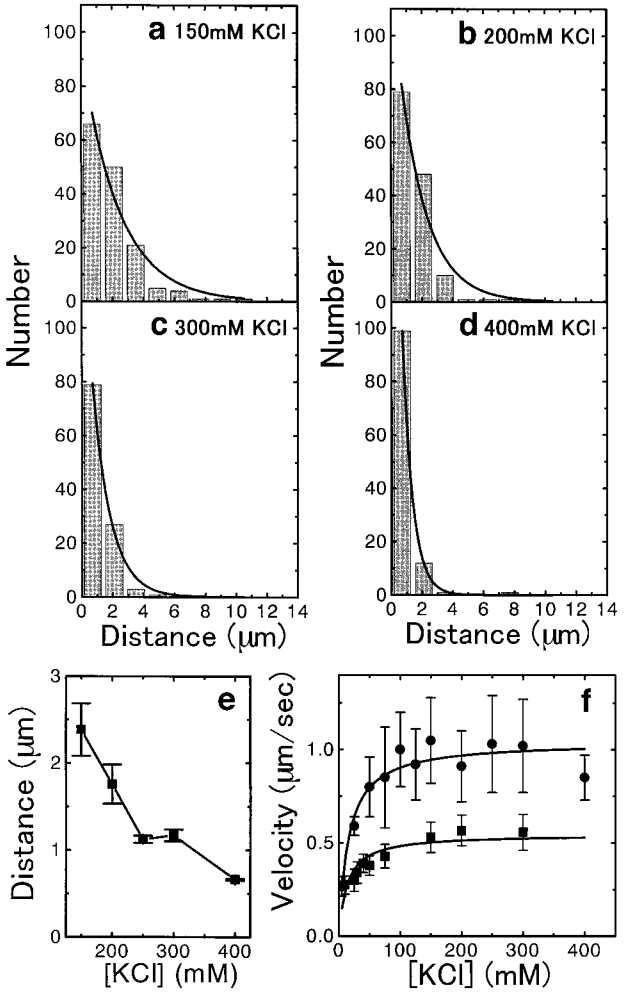

FIG. 3. Processive movement by individual BMV molecules at various ionic strengths. (a–d) Distribution of distances traveled on actin tracks by individual BMV molecules before detachment. Solid curves: exponential fits with length constants, 2.39 μm (a), 1.76 μm (b), 1.17 μm (c), and 0.66 μm (d). The average travel distances are plotted as a function of [KCl] in (e). (f) The rate, as a function of [KCl], of actin-filament translation propelled by large ensembles of BMV (closed squares), and the rate, as a function of [KCl], of processive movement by individual BMV molecules along their actin tracks (closed circles).

[KCl], and reached a plateau (1 μm/s) at about 150 mM KCl (Fig. 3f). This behavior is different from that of kinesin. The rate of processive movement of kinesin is independent of ionic strength (15).

The actin-activated BMV and Cy3-BMV ATPase activities were measured in 2 mM ATP and three different [KCl] with various concentrations of actin. The results are summarized in Table 1. The ATPase activities displayed simple hyperbolic saturation behavior as a function of [actin] (data not shown), i.e., $V_{max}/(1 + K_m^A/[actin])$. Irrespective of [KCl] both samples exhibited similar maximum turnover rates, V_{max} ($\sim$2.4 s^{-1}). They also showed similar K_m^A. These values agreed with those reported previously for native BMV (23). These results, together with the same rate of actin translocation propelled by BMV and Cy3-BMV, guarantee that the CaM-exchange does not alter the properties of BMV. The rate of movement (0.54 μm/s at 25 mM KCl, 1 μm/s at [KCl] higher than 150 mM) of single Cy3-BMV molecules and the ATPase turnover rate (2.4 s^{-1}) suggest that Cy3-BMV may travel a great distance (230–400 nm) per an ATPase cycle, although it does not prove. To accommodate the maximum rate of movement (1 μm/s) with the step size (ca. 36 nm) observed by an optical trapping assay with native BMV in the absence of Ca^{2+} and in various [ATP] (12), we may be able to consider two hypothetical cases. Case 1: The 36 nm step is not directly coupled with each ATPase cycle. Within one ATPase cycle, BMV could make multiple (6–11) 36 nm-step advances in succession, as has been suggested with skeletal muscle myosin subfragment-1 (24). This view may be supported by an observation that dwell durations between 36 nm-steps were much shorter than the ATPase cycle time (12). If so, the dwell durations should be insensitive to [ATP], as long as 'rigor head' formed in low [ATP] does not hinder its nucleotide-bound partner from repeating 36 nm-steps in succession. However, observed dwell durations increased with decreasing [ATP] (12). Case 2: A large fraction (more than 90%) of BMV may be in an inhibited or low-activity state where it does not interact with actin, and therefore BMV not in such a state may have much higher ATPase activity (14 s^{-1}/head, or 28 s^{-1}/BMV), 12 times larger than the value measured here. If so, it is understandable that large ensembles of BMV molecules produced actin-filament sliding at a rate half that with movement of single BMV molecules. We tested this hypothesis by cosedimentation assays for BMV and Cy3-BMV binding to F-actin in 2 mM ATP. It came out that this hypothesis did not fit, because a large fraction of BMV and Cy3-BMV were cosedimented with F-actin, even at 150 mM KCl (Fig. 4). This cosedimentation does not mean that our BMV sample contains a large fraction of denatured BMV, but that BMV is mainly in the strong-binding states during the ATPase cycle (13, 14). If denatured, it must produce resistive drag force against actin-filament sliding, as has been observed with skeletal heavy meromy-

TABLE 1

Steady-State ATPase Rate of Acto-BMV and Acto-Cy3-BMV at Three Different KCl Concentrations

KCl (mM)	V_{max} (s^{-1})		K_m^A (μM)	
	BMV	Cy3-BMV	BMV	Cy3-BMV
25	2.37	2.41	0.39	0.41
100	2.20	2.36	1.10	1.28
200	2.47	2.42	7.09	7.00

Note. V_{max}, the maximum ATPase rate; K_m^A, actin concentration where the ATPase rate is half of V_{max}.

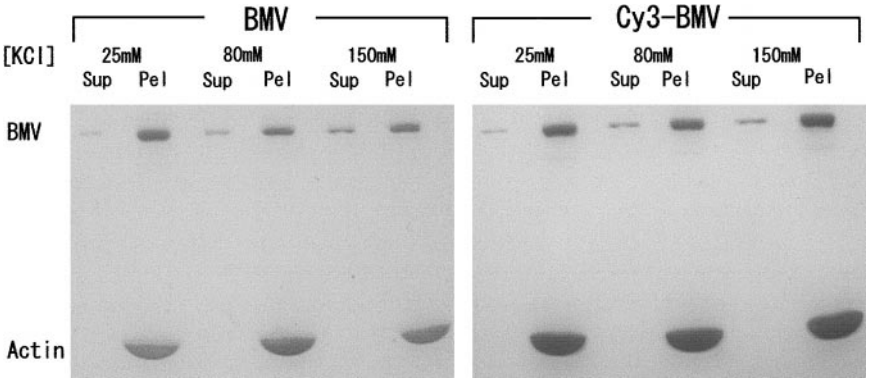

FIG. 4. Greyscale ccd images of silver-stained SDS-gels from F-actin cosedimentation assays. Left panel, BMV (150 nM), and right panel, Cy3-BMV (150 nM), were incubated with 40 μM F-actin in the presence of 2 mM ATP and three different [KCl] (25 mM, 80 mM, 150 mM). Pell, 20 μl sample of pellets resuspended in the original volume of the buffer solution was loaded. Sup, 20 μl sample of supernatants, were loaded. The silver-staining conditions are slightly different between left and right panels.

osin, wherein only 15–20% denatured fraction of heavy meromyosin is sufficient to stop actin-filament sliding. The ATPase activity as high as 14 s^{-1}/head has been reported for native BMV in the presence of a micromolar order of Ca^{2+} (23) and for truncated, single-headed myosin V constructs with one or two single light chains in the absence of Ca^{2+} (13, 25). The high ATPase activities are, however, ascribed to the absence of an inhibitory effect of CaM on the acto-BMV ATPase reaction (23). Without the inhibitory effect of CaM, BMV does not support *in vitro* motility of actin filaments (10).

Here, we provided hard evidence that BMV is a highly processive motor that can travel over a distance of many micrometers without detaching from actin. However, it raised a new riddle about the mechanochemical coupling of this protein motor, which should be solved in the future.

ACKNOWLEDGMENTS

We thank K. Saito for the OTIRF microscope. This work was supported partly by the Ministry of Education, Science, Sports and Culture of Japan (Grant-in-Aid for Scientific Research on Priority Areas (A) to T.A.) and by the Sasagawa Scientific Research Grant from The Japan Science Society to T.S.

REFERENCES

1. Prekeris, R., and Terrian, D. M. (1997) *J. Cell Biol.* **137,** 1589–1601.
2. Evans, L. L., Lee, A. J., Bridgman, P. C., and Mooseker, M. S. (1998) *J. Cell Sci.* **111,** 2055–2066.
3. Tabb, S., Molyneaux, B. J., Cohen, D. L., Kuznetsov, S. A., and Langford, G. M. (1998) *J. Cell Sci.* **111,** 3221–3234.
4. Provance, D. W., Wei, M., Jr., Ipi, V., and Mercer, J. A. (1996) *Proc. Natl. Acad. Sci. USA* **93,** 14554–14558.
5. Wu, X. F., Bowers, B., Wei, Q., Kocher, B., and Hammer, J. A. (1997) *J. Cell Sci.* **110,** 847–859.
6. Hill, K. L., Catlett, N. L., and Weisman, L. S. (1996) *J. Cell Biol.* **135,** 1535–1549.
7. Catlett, N. L., and Weisman, L. S. (1998) *Proc. Natl. Acad. Sci. USA* **95,** 14799–14804.
8. Espindola, F. S., Esprefico, E. M., Vcoelho, M., Martins, A. R., Casta, F. R. C., Mooseker, M. S., and Larson, R. E. (1992) *J. Cell Biol.* **118,** 359–368.
9. Esperafico, E. M., Cheney, R. E., Matteoli, M., Nascimento, A. A. C., De Camilli, P. V., Larson, R. E., and Mooseker, M. S. (1992) *J. Cell Biol.* **119,** 1541–1557.
10. Cheney, R. E., O'shea, M. K., Heuser, J. E., Coelho, M. W., Wolonski, J. S., and Espreafico, E. M. *Cell* **75,** 13–23.
11. Cameron, L. C., Carvalho, R. N., Araujo, J. R. V., Santos, A. C., Tauhata, S. B., Larson, R. E., and Sorenson, M. M. (1998) *Arch. Biochem. Biophys.* **355,** 35–42, doi:10.1006/abbi.1998.0700.
12. Mehta, A. D., Rock, R. S., Rief, M., Spudich, J. A., Mooseker, M. S., and Cheney, R. E. (1999) *Nature (London)* **400,** 590–593.
13. De La Cruz, E. M., Wells, A. L., Rosenfeld, S. S., Ostap, E. M., and Sweeney, H. L. (1999) *Proc. Natl. Acad. Sci. USA* **96,** 13726–13731.
14. Titus, M. A. (1997) *Curr. Biol.* **7,** R301–R304.
15. Vale, R. D., Funatu, T., Pierce, D. W., Romberg, L., Harada, Y., and Yanagida, T. (1996) *Nature (London)* **380,** 451–453.
16. Howard, J., Hudspeth, A. J., and Vale, R. D. (1989) *Nature (London)* **342,** 154–158.
17. Sakakibara, H., Kojma, H., Sakai, Y., Katayama, E., and Oiwa, K. (1999) *Nature (London)* **400,** 586–590.
18. Cheney, R. E. (1998) *Methods Enzymol.* **298,** 3–18.
19. Kunioka, Y., and Ando, T. (1996) *J. Biochem.* **119,** 1024–1032.
20. Toyoshima, Y. Y., Kron, S. J., McNally, E. M., Niebling, K. R., Toyoshima, C., and Spudich, J. A. (1987) *Nature (London)* **328,** 536–539.
21. Tokunaga, M., Kitamura, K., Saito, K., Iwane, A. H., and Yanagida, T. (1997) *Biochem. Biophys. Res. Commun.* **235,** 47–53, doi:10.1006/bbrc.1997.6732.
22. Fiske, C. H., and Subbarow, Y. (1925) *J. Biol. Chem.* **14,** 1–10.
23. Nascimento, A. A. C., Cheney, R. E., Tauhata, S. B. F., Larson, R. E., and Mooseker, M. S. (1996) *J. Biol. Chem.* **271,** 17561–17569.
24. Kitamura, K., Tokunaga, M., Iwane, A. H., and Yanagida, T. (1999) *Nature (London)* **397,** 129–134.
25. Trybus, K. M., Krementsova, E., and Freyzon, Y. (1999) *J. Biol. Chem.* **274,** 27448–27456.